DAMAGE ANALYSIS OF ULTRALIGHT COMPOSITE SANDWICH STRUCTURES

Julien Rion, Yves Leterrier, Fabio Demarco, Jan-Anders E. Månson
Laboratoire de Technologie des Composites et Polymères (LTC)
Ecole Polytechnique Fédérale de Lausanne (EPFL), CH-1015 Lausanne, Switzerland

Keywords: *sandwich, honeycomb, peel test, adhesive weight*

Abstract

The failure mechanisms during peeling of the skin of ultralight sandwich structure (<1kg/m^2) with honeycomb core were studied. Tearing energy of honeycomb core was first measured. To this end a modified double cantilever beam test and a video crack measurement system coupled with an elastic foundation model were developed. This method allowed quick measurement of the tearing energy and gave the same results as the classical time-consuming compliance calibration method.

The peeling energy of the skin of the sandwich structure was then measured with climbing drum peel test with different amounts of adhesive for skin to core bonding. Two different regimes have been observed, with transition between cohesive failure of the resin fillet and tearing of honeycomb. The measured tearing energy of honeycomb was found to correspond well to peeling energy measured when honeycomb tore.

1 Introduction

Composite sandwich structures are used in all applications requiring high strength and stiffness with low weight. In the frame of the ultralight solar airplane project currently ongoing at EPFL, the sandwich structures have to be pushed to the limits to save as much weight as possible. Therefore, each component of the sandwich structure, namely the skins, the core and the skin-core adhesive have to be selected carefully. The lightest honeycomb core and very thin skins are therefore used. This structure has then to be optimized in terms of stiffness and strength to weight ratio in order to save a maximum of weight.

The optimization of sandwich structures has been considered by numerous authors. For example, Froud [1] and later Theulen and Peijs [2] optimized the weight ratio between skin and core, but only considering face failure. Triantafillou and Gibson [3] considered different failure modes of foam core sandwich beams. They determined analytically failure criteria and then established failure maps to determine type of failure in function on sandwich design. They confirmed that the structure with best strength to weight ratio is obtained when the different failure types occur simultaneously. However they didn't consider core/skin delamination.

In order to get optimal structure, criteria for every failure modes have to be developed. For light sandwich structures, skin debonding is certainly the less mastered failure mode. It is easy to avoid by putting enough adhesive, but as weight has to be saved, the lower limit has to be found. Therefore, this study especially concentrates on skin to core bonding.

Resin fillet formation is known to considerably impact the efficiency of the bonding [4-6] and this study concentrated on the influence of the resin meniscus geometry on mechanical strength and failure modes. As it was shown that the core can be torn when the bonding is sufficient [7], the honeycomb core was first characterized independently. The skin/core debonding mechanisms were subsequently analyzed on sandwich structures.

2 Materials and methods

2.1 Tearing energy of honeycomb cores

Honeycomb is a cellular material, but tearing energy per unit surface was calculated as for a continuous solid material. The energy required to propagate a crack through the honeycomb core in mode 1 (crack opening mode), was measured with a modified double cantilever beam test (DCB).

The honeycomb was a Nomex honeycomb from Hexcel, with hexagonal cell of 3.2 mm diameter and a weight of 29 kg/m^3. The samples were made of 8 mm thick, 20 mm wide and 200 mm long honeycomb samples, cut in ribbon direction. The honeycomb was glued between 2 plates of 2 mm thick glass fibers / epoxy composite. The adhesive film used was 150 g/m^2 from Advanced Composite Group (ACG VTA 260 adhesive film). Two small aluminum blocks with a hole were glued on one end of the sample to introduce the load. A crack was initiated with a cutter in the middle of the honeycomb. The two arms were then pulled apart with 2 mm/min and the crack propagated in the honeycomb. The load and crosshead displacement were recorded during the test.

The critical point of this test was to measure crack length. Indeed, as Nomex honeycomb is tough, the honeycomb tears progressively and the crack tip can hardly be localized by visual observation. Therefore, a compliance calibration method and a new method based on video acquisition and analysis of the deformed sample were used to measure the crack.

For the compliance calibration method, a crack of controlled length was cut in the honeycomb. The tip of the crack was marked with a pen. The sample was loaded to the beginning of the crack propagation, easily identifiable by hearing the acoustic emissions. Crosshead was stopped at this time and the distance between loading line and marked crack tip was measured (Fig. 1). This corrected crack length is smaller than the real length of the cracked zone. But it has been shown by Williams [8] that by using this length, no correction factors are necessary for large displacement, as it corresponds to the true distance for moment calculation at crack tip. The slope of the load deformation curve was measured and the compliance C was calculated for this crack length. This procedure was conducted for crack length between 40 and 120 mm. Five measurements were made on each of the six samples. The function correlating the compliance and crack length was then determined.

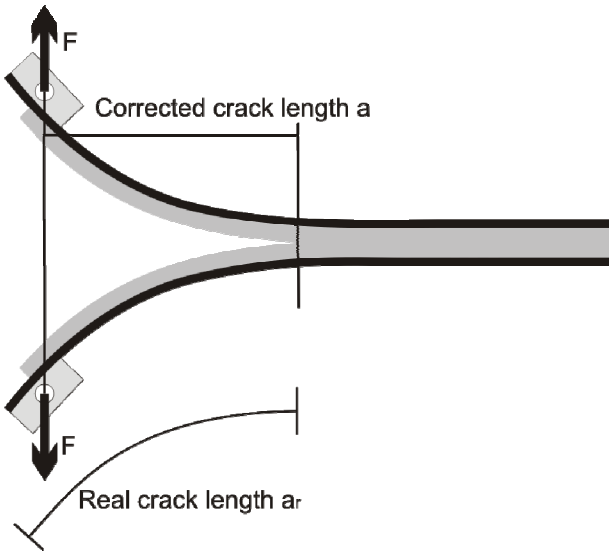

Fig. 1. Schema of the DCB test specimen with the corrected crack length which has to be used to calculate G_c

Classical beam theory for a perfectly clamped beam with end load will give the relation

$$C = \frac{\delta}{F} = Da^3 \qquad (1)$$

where δ is the displacement of the loading point, D a coefficient depending of beam geometry and material, F the applied load and a the distance between loading line and clamped end. As in the DCB test, the end can not be considered as perfectly clamped due to honeycomb elasticity, a correction has to be established. The compliance calibration method (CC) and the modified beam theory (MBT) [9] are the most often used corrections methods.

Compliance calibration method uses a correction factor considering that

$$C = \frac{\delta}{F} = Da^n \qquad (2)$$

where n is fitted to the experimental results. Therefore, a graph representing *log(C)* in function of *log(a)* is constructed and the slope directly gives the exponent n. The tearing energy G can then be directly calculated.

With Griffith theory [10], the strain energy release rate for an infinitesimal increase in crack length da under constant displacement is

$$G = -\frac{1}{B}\frac{dU}{da}\bigg|_{\delta=const.} \qquad (3)$$

where U is the total elastic strain energy in the test specimen and B the sample width. This can be written as

$$G = \frac{F^2}{2B}\frac{dC}{da} \tag{4}$$

Using Eq. 2 and 4, we can directly obtain

$$G = \frac{F^2}{2B} nD \left(\frac{C}{D}\right)^{\frac{n-1}{n}} \tag{5}$$

With Eq. 5, once the coefficients D and n are determined, the strain energy release rate can be calculated without measuring a, what is very advantageous to make tests. This method has been successfully used by Berkowitz and Johnson [7]. They measured critical strain energy release rate during delamination of a sandwich structure with 48 kg/m^3 Nomex honeycomb core and carbon fibers faces. In every samples the failure was honeycomb tearing, with G_C = 1180 J/m^2 at room temperature.

In the modified beam theory, correction is made by introducing a slightly longer crack length $a + \Delta$. From Eq. 1 and 3, we obtain

$$G = \frac{3F\delta}{2Ba} \tag{6}$$

which becomes for MBT

$$G = \frac{3F\delta}{2B(a+\Delta)} \tag{7}$$

The calculation of the value of Δ can be made empirically as described in the standards for the modified beam theory method [9] or by considering a beam on elastic foundation similarly as described by Williams [11] for DCB test on laminates.

In contrary to the CC method, MBT requires to know the value of a during the test. A method was developed to measure crack length during the test on the DCB sample. A video camera takes pictures of the sample being tested. A black background is used to have a good contrast with the peel arms (Fig. 2). The images are then treated in real time by a NI Labview program to measure the vertical distance between the two peel arms. A mean distance in the uncracked region is calculated and according Eq. 1, a third order polynomial is fitted to the vertical distance measured in the cracked zone. The intersection between the third order polynomial of cracked zone and the mean of the uncracked zone gives the location of the crack tip.

The two methods described above need to measure the compliance of the system with many different crack lengths to be able to calculate accurately the correction factors n respectively Δ. To avoid these time consuming experiments it is possible to develop an analytical model to predict compliance in function of the properties of the material constituting the sample. The basis idea is to consider that the two arms of the DCB sample are not perfectly clamped, but are laid on an elastic foundation (Fig. 3). The elastic foundation is considered as linear springs, so that the line load $q(z)$ is

$$q(z) = -K \cdot y(z) \tag{8}$$

with

$$K = \frac{EB}{t_c/2} \tag{9}$$

where E is the tensile modulus of honeycomb, and t_c the thickness of the core. For equilibrium for $0 < z < d$, we have

$$D_B \cdot y''(z) = \int_0^z -k \cdot (z-t) \cdot y(t)\, dt \tag{10}$$

where D_B is the bending stiffness of the peel arm. The integral can be considered as a convolution product and Laplace Transform allows obtaining

$$Y(s) = \frac{s^3 \cdot y(0) + s^2 \cdot y'(0)}{s^4 + \kappa^4} \tag{11}$$

with

$$\kappa^4 = \frac{K}{D_B} \tag{12}$$

The inverse Laplace Transform gives then

$$y(z) = \frac{Cosh\left[\frac{\kappa z}{\sqrt{z}}\right]}{2\kappa} \left(\left(2\kappa y(0) Cos\left[\frac{\kappa z}{\sqrt{z}}\right] + \sqrt{2} y'(0) Sin\left[\frac{\kappa z}{\sqrt{z}}\right]\right) + \sqrt{2} y'(0) Cos\left[\frac{\kappa z}{\sqrt{z}}\right] Sinh\left[\frac{\kappa z}{\sqrt{z}}\right]\right) \tag{13}$$

The equilibrium conditions also give

$$\int_0^d K \cdot y(z) dz = F$$
$$\int_0^d K \cdot z \cdot y(z) dz = F(a+d) \tag{14}$$

where d is the length of the elastic foundation, i.e. the length of the uncracked part of the sample

(Fig. 3). By solving the equations, we obtain the slope and displacement for z = 0

$$y(0)=\frac{2F\kappa}{K\left(-2+Cos\left[\sqrt{2}d\kappa\right]+Cosh\left[\sqrt{2}d\kappa\right]\right)}$$
$$\left(\sqrt{2}Cos\left[\frac{\kappa d}{\sqrt{2}}\right]Sinh\left[\frac{\kappa d}{\sqrt{2}}\right]\right.$$
$$\left.-Sin\left[\frac{\kappa d}{\sqrt{2}}\right]\left(\sqrt{2}Cosh\left[\frac{\kappa d}{\sqrt{2}}\right]+2a\kappa Sinh\left[\frac{\kappa d}{\sqrt{2}}\right]\right)\right)$$
$$y'(0)=\frac{2F\kappa^2}{K\left(-2+Cos\left[\sqrt{2}d\kappa\right]+Cosh\left[\sqrt{2}d\kappa\right]\right)} \quad (15)$$
$$\left(\sqrt{2}a\kappa Cosh\left[\frac{\kappa d}{\sqrt{2}}\right]Sin\left[\frac{\kappa d}{\sqrt{2}}\right]\right.$$
$$\left.+Sinh\left[\frac{\kappa d}{\sqrt{2}}\right]\left(\sqrt{2}a\kappa Cos\left[\frac{\kappa d}{\sqrt{2}}\right]+2Sin\left[\frac{\kappa d}{\sqrt{2}}\right]\right)\right)$$

With Eq. 15 and 13, the slope and displacement at $z = d$ can be calculated. Then for $d < z < d + a$, we have

$$y(z)=\frac{F}{2D_B}\left(a(z-d)^2-\frac{1}{3}(z-d)^3\right)+y'(d)(z-d)+y(d) \quad (16)$$

and finally the compliance can be calculated as

$$C(a)=\frac{y(a+d)}{F} \quad (17)$$

By knowing $C(a)$, G can be calculated either by using directly Eq. 4 or by calculating Δ so that

$$\frac{F(a+\Delta)^3}{3D_B}=y(a+d) \quad (18)$$

and then using Eq. 7.

For the numerical application, D_B has been measured with 3-points bending test on a peel arm of broken DCB sample. The Young's modulus E of the honeycomb has been measured by pulling apart honeycomb as for flatwise tensile test and measuring the strain.

For the measurement of G, the crack was propagated in 3 steps, from 50 mm to 70 mm, 70 mm to 90 mm and from 90 mm to 110 mm, to allow adjusting the zoom of the camera to have most accurate measurements. These successive loading cycles also allow calculating the energy used to propagate the crack by integrating the area under the curve (Fig. 4). As all the deformations are elastic, all the energy dissipated during the loading cycle is due to crack propagation. The mean G value can then be calculated as

$$G=\frac{\Delta U}{\Delta a_r} \quad (19)$$

where a_r is the real crack length as represented in Fig. 1.

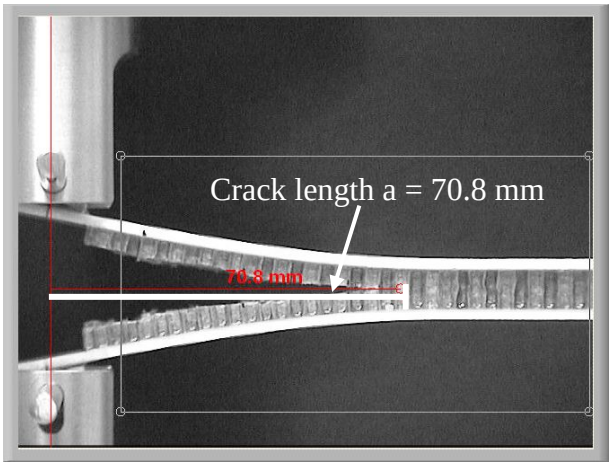

Fig. 2. Image of the sample with the video camera. The program calculates and shows corresponding crack length

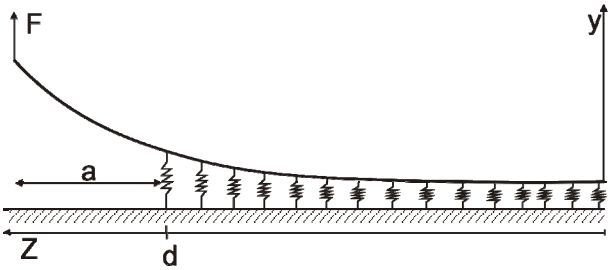

Fig. 3. Basic scheme of a DCB arm on elastic foundation. At $z = 0$, the moment and the shear force are zero.

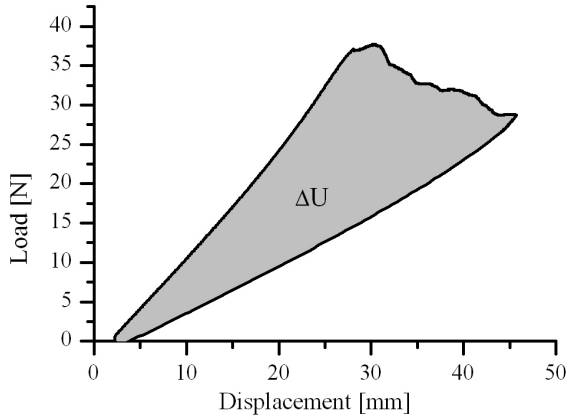

Fig. 4. Load displacement curve recorded during DCB crack propagation. The energy used for the crack propagation is ΔU.

2.2 Peeling energy of sandwich structures

In order to measure the debonding energy of the skin, climbing drum peel test was used as it is the most appropriate test in mode 1 for sandwich with very thin skins [12]. Sandwich samples with 0.2 mm thick unidirectional carbon fiber skins and 8 mm thick, 29 kg/m^3 Nomex honeycomb core were produced. The adhesive used was a VTA 260 epoxy resin system from Advanced Composite Group. The adhesive was deposited on honeycomb with controlled weight in the range from 8 to 100 g/m^2 as described by Rion et al. [13]. Core and skin were bonded under vacuum.

The samples for the climbing drum peel test were 70 mm wide. The peel direction was the ribbon direction of honeycomb. The test was conducted in two steps. Firstly, the carbon skin was peeled off the sandwich during a first climb of the drum and the force-displacement data was recorded. Immediately after this first climb, a second climb was realized with the same structure, but with debonded skin. The force recorded during this second step gave the part necessary to make the drum climb and to bend the skin, which was subtracted from the total force measured in first step. The debonding energy of the skin was subsequently calculated as

$$G_{IC} = \frac{(F_{peak} - F_o)(r_o - r_i)}{Wr_i} \qquad (20)$$

where F_{peak} is the average peak load, F_o is the force to make the drum climb and to bend the skin, r_o and r_i are the outer and inner diameters of the drum and W is the sample width.

In order to characterize the failure mode of the structure, micrographs of the bonding fillet were taken after peel test on Olympus BX-61 microscope.

3 Results and discussion

3.1 Tearing energy of honeycomb

The load-displacement curves measured with different crack length confirmed the hypothesis of linear elastic behavior of the DCB sample until crack growth (Fig. 5). When a sharp crack is created with a razor blade, the opening force does not decrease when crack starts propagating. This is due to the toughness of honeycomb. Indeed, the failure process corresponds more to progressive tearing of the honeycomb than real crack propagation. The force-displacement curve can then be separated in different regimes. Firstly, the linear behavior where no tearing takes place can be used to calculate compliance. Then the tearing zone forms between non linearity point of the curve and maximum load. Finally, the tearing zone propagates and the force decreases. The tearing energy is calculated during this third regime.

The compliance corresponding to various crack length can then be measured and the coefficients D and n can be calculated. The correspondence between the fitted curve and the experimental data is very good (Fig. 6), what demonstrates the validity of Eq. 2. G can then be calculated only by measuring the force during crack propagation, as described by Eq. 5.

The compliance predicted with the elastic foundation model corresponds well to the experimental data, with a slight under estimation for large crack length (Fig. 6). As the calculation of G is made with crack length smaller than 100 mm to avoid too large deformations of the peel arms, the model corresponds well in the needed range.

The value of Δ calculated with this model to use Eq. 7 varies only slightly with crack length, between 8.74 mm for a = 40 mm and 8.70 mm for a = 100 mm.

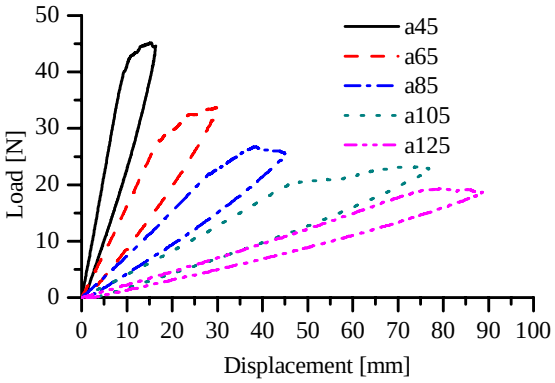

Fig. 5. Measurement of compliance with different crack lengths from 45 to 125 mm. The DCB sample is loaded until crack begins to propagate and then unloaded. The crack is then propagated artificially with a razor blade. The slope of the loading curve allows calculating the compliance corresponding to the crack length.

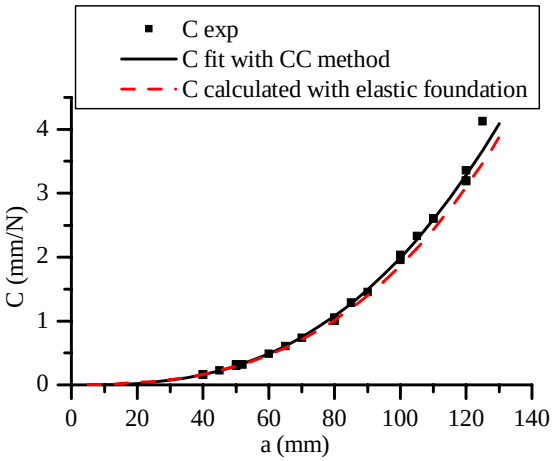

Fig. 6. Prediction of compliance in function of crack length with compliance calibration method and elastic foundation model.

For the measurement of *G*, the crack was propagated in 3 steps, from 50 to 70 mm, from 70 to 90 mm and finally from 90 to 110 mm. Fig. 7 illustrates the second propagation. The crack was 70 mm length at the beginning of the test. As the crack was created by loading the DCB sample and not with razor blade, the tearing zone was already created. Therefore the propagation of the tearing zone begins directly after the linear regime and the maximum force is obtained at the end of the linear regime and corresponds well to the beginning of the measured crack growth.

The measurements of the crack length with the video system correspond very well to the crack length calculated with the compliance calibration method. The video system allows avoiding the time consuming compliance calibration procedure.

For each sample, the *G* value has been calculated during the propagation of the tearing zone, i.e. from maximum load to the unloading. A mean value has been calculated then for each measurement. The different calculation methods give very similar results with maximum difference smaller than 3% (Table 1). According to the standards [9], MBT method gives the most conservative result. The direct use of the compliance calculated with the elastic foundation model gives an intermediate value between MBT and CC method. The use of the elastic foundation model coupled with the video system measurement allows then to calculate quickly the G_C value without making the numerous measurements necessary for the compliance calibration. The result obtained by integration of the energy dissipated gives slightly higher energy, but the difference is comprised in the standard deviation and is not significant.

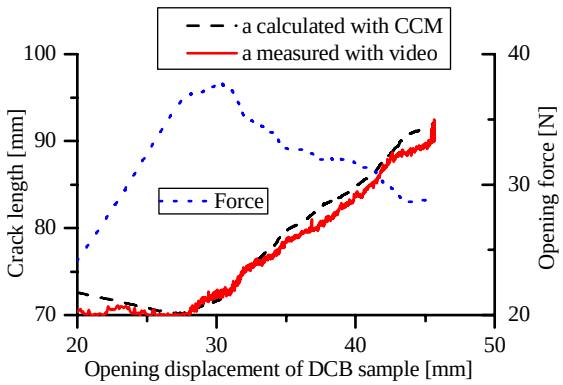

Fig. 7. Crack length *a* measured with video system and calculated with CC method. Crack length before loading was 70 mm. In contrary to Fig. 5, the crack before this test was created by loading the DCB sample and propagating the crack to 70mm.

Table 1. Critical strain energy release rate G_C for crack propagating in honeycomb calculated with various methods.

Calculation method	**G [J/m^2]** ***Average***	***Standard deviation***
Compliance calibration method (Eq. 5)	1009	71
Modified beam theory (Eq. 7), Δ from elastic foundation model	996	69
Definition formula (Eq. 4), C from elastic foundation model	998	71
Crack propagation energy measurement (Eq. 19)	1025	66

3.2 Peeling energy of sandwich structures

During the climbing drum peel test, the force displacement curve presents a saw tooth shape (Fig. 8). This is due to the discontinuity of the honeycomb core. Each tooth corresponds to a crack propagation of the length of one honeycomb cell. For the calculation of the critical crack energy release rate (G_{IC}), the average of the peak loads has been considered.

The curve showing the critical crack energy release rate in function of adhesive weight presents clearly two different slopes. A fast increase of G_{IC} from 0 to 40 g/m^2 adhesive is followed by a slower increase above this value (Fig. 9).

The micrographs taken from the samples after the peel test allow identifying different failure modes. From 0 to 40 g/m^2, cohesive failure of the adhesive fillets is the dominant mode (Fig. 10). As the fracture energy is proportional to the fracture surface, the G_{IC} value increases quickly with adhesive weight.

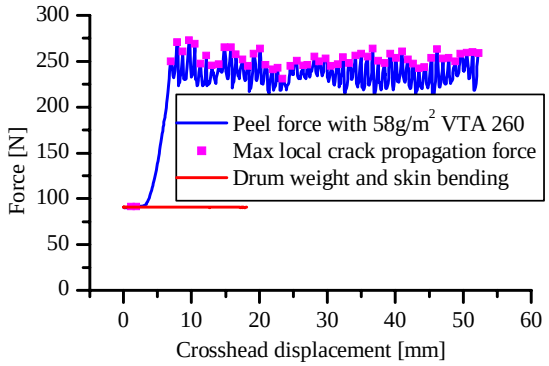

Fig. 8. Force displacement curve recorded during skin peeling. The force needed to peel the skin is the difference between total force recorded and the force needed to make the drum climb and to bend the skin

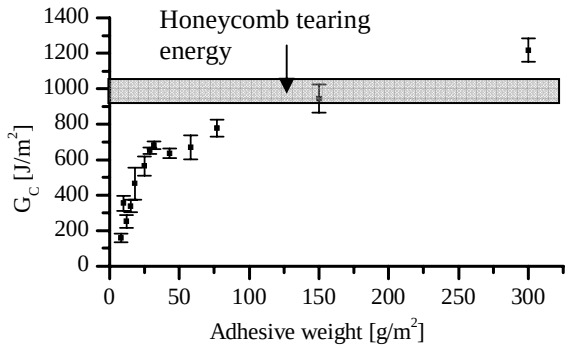

Fig. 9. Skin debonding energy in function of adhesive weight

Above 40 g/m^2 adhesive, the driving failure type is honeycomb tearing (Fig. 11). As the adhesive quantity increases, small adhesive amount climbs along honeycomb cell walls due to capillarity forces, what reinforces slightly the core. This explains the slow increase of G_{IC} with adhesive amount above 40 g/m^2. Furthermore, with large amount of adhesive, the failure occurs above the resin meniscus, which is in the order of 1 mm height. To exactly calculate the G_{IC} value, the r_i value in Eq. 20 should be increased by fillet height, what would slightly diminish G_{IC}. As this effect is not taken in account in Fig. 9, it also explains the increasing value above 40 g/m^2.

The debonding energy measured with 150 g/m^2 adhesive corresponds well to the tearing energy of honeycomb. This shows then that the upper limit of the peeling strength of sandwich structures with very light core can be predicted by measuring the tearing strength of the core. This can then be a useful value to evaluate the maximal peeling energy affordable with a given core.

The main interest for such light structures is to get the best strength to weight ratio. The ratio between peeling energy and adhesive weight shows a maximum at about 35 g/m^2, i.e. at the transition between the to failure modes (Fig. 12). This adhesive quantity can then be considered as the optimal value for peeling loading case. As peeling is the most sever loading case for such bonding, this optimum value can then be considered as an upper limit for other loading cases.

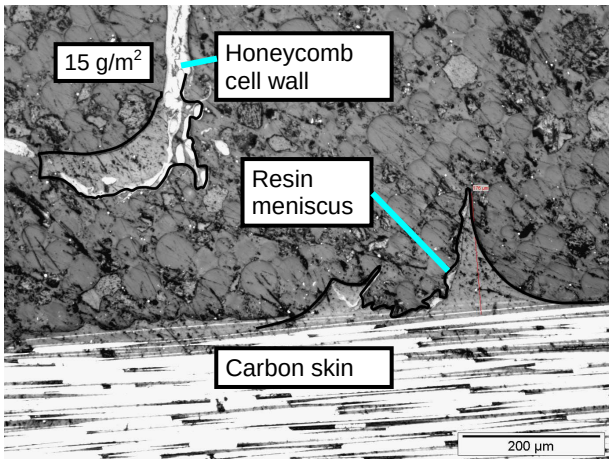

Fig. 10. Micrograph of a cross-section of a sandwich sample with 15 g/m^2 adhesive after peel test. The failure is due to cohesive failure of the resin. The surface of the meniscus has been highlighted with black line for better legibility

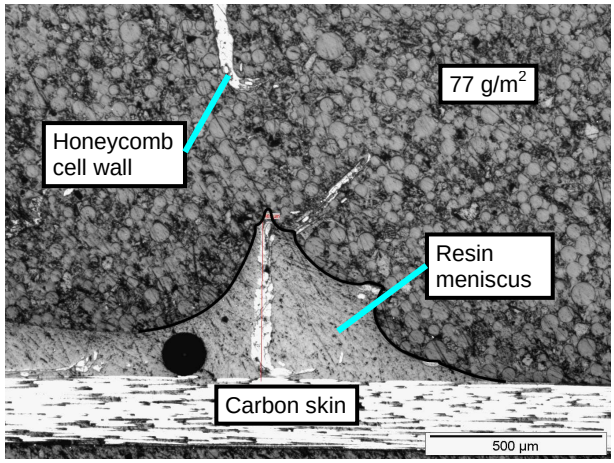

Fig. 11. Micrograph of a cross-section of a sandwich sample with 77 g/m^2 adhesive after peel test. The failure is due to tearing of the honeycomb. The surface of the meniscus has been highlighted with black line for better legibility

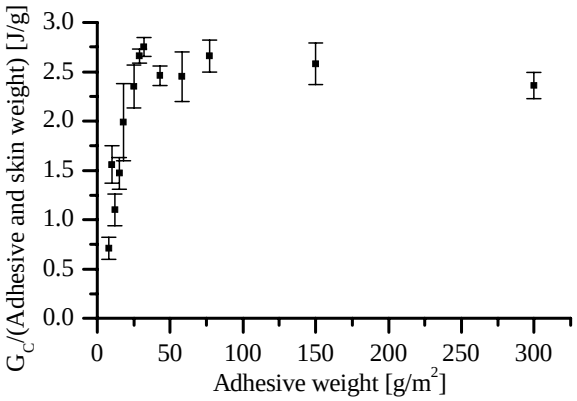

Fig. 12. G_{IC} to adhesive weight ratio, in function of adhesive weight. The maximum value is at about 35 g/m^2.

4 Conclusions

The failure of ultralight sandwich samples under peeling load was investigated, with attention paid to the influence of resin fillets between honeycomb core and skin. Firstly, the tearing energy of the honeycomb core was measured to predict the maximum peel strength. A modified DCB test was used to this end and a new method was developed to measure the crack length, based on deformation analysis of the peeling arms. Coupled

with the elastic foundation model developed in this work, the tearing energy was measured quickly and accurately and found to be equal to 998 J/m^2, as confirmed with the more classical but time consuming compliance calibration method.

Secondly, climbing drum peel tests were conducted on sandwich samples with various core/skin adhesive quantities. Two different failure modes were identified. Below 40 g/m^2, cohesive failure of the resin fillet occurs, and the debonding energy increases quickly with adhesive weight. Above 40 g/m^2, tearing of honeycomb core occurs and the debonding energy increases only slowly with adhesive weight. It was shown that the optimal adhesive weight to obtain the best strength to weight ratio is at the failure mode transition point, i.e. at ~35 - 40g/m^2.

It could also be observed that the tearing energy of honeycomb corresponds well with the peeling energy of the sandwich sample with 150 g/m^2 adhesive, and thus can be used as upper limit for the peeling energy of the sandwich.

Acknowledgements

The authors want to thank EPFL and the Swiss Commission for Technology and Innovation (CTI, #8002.1;3 DCPP-NM) for financial support.

References

[1] Froud G.R. "Your sandwich order, Sir?" *Composites*, Vol. 11, No. 3, pp 133, 1980.

[2] Theulen J.C.M. and Peijs A.A.J.M. "Optimization of the bending stiffness and strength of composite sandwich panels". *Composite Structures*, Vol. 17, No. 1, pp 87, 1991.

[3] Triantafillou T.C. and Gibson L.J. "Failure mode maps for foam core sandwich beams". *Materials Science and Engineering*, Vol. 95, pp 37-53, 1987.

[4] Chanteranne J. "Use of ultra-light adhesive for the metal-honeycomb bonding". *Annales de Chimie-Science des Matériaux*, Vol. 12, No. 2, pp 199-204, 1987.

[5] Grove S.M., Popham E. and Miles M.E. "An investigation of the skin/core bond in honeycomb sandwich structures using statistical experimentation techniques". *Composites Part A-Applied Science and Manufacturing*, Vol. 37, No. 5, pp 804-812, 2006.

[6] Okada R. and Kortschot M.T. "The role of the resin fillet in the delamination of honeycomb sandwich structures". *Composites Science and Technology*, Vol. 62, No. 14, pp 1811-1819, 2002.

[7] Berkowitz C.K. and Johnson W.S. "Fracture and fatigue tests and analysis of composite sandwich structure". *Journal of Composite Materials*, Vol. 39, No. 16, pp 1417-1431, 2005.

[8] Williams J.G. "Large displacement and end block effects in the DCB interlaminar test in mode-I and mode-II". *Journal of Composite Materials*, Vol. 21, No. 4, pp 330-347, 1987.

[9] "ASTM D 5528-94a, standard test method for mode 1 interlaminar fracture toughness of unidirectionnal fiber-reinforced polymer matrix composites". *Annual Book of ASTM Standards*, Vol. 15.03, 1994.

[10] Labbens R. "*Introduction à la mécanique de la rupture"*. Editions Pluralis, 1980.

[11] Williams J.G. "End corrections for orthotropic DCB specimens". *Composites Science and Technology*, Vol. 35, No. 4, pp 367-376, 1989.

[12] "ASTM D 1781-98, standard test method for climbing drum peel for adhesives". *Annual Book of ASTM Standards*, Vol. 15.06, 1998.

[13] Rion J., Geiser A., Leterrier Y. and Månson J.-A. "Ultralight composite sandwich structure: Optimization of skin to honeycomb core bonding". Proceedings of 27th International Conference of SAMPE Europe, Paris, 2006.